

Graph-based Detection of Multiuser Impulse Radio Systems

Yehuda Shen Bahar and Ofer Amrani
 School of Electrical Engineering,
 Dept. Elec. Eng. - systems,
 Tel-Aviv University, Tel-Aviv, Israel
 yeuda,ofera@eng.tau.ac.il, +972-3-6407766

Abstract - Impulse-Radio (IR) is a wideband modulation technique that can support multiple users by employing random Time-Hopping (TH) combined with repeated transmissions. The latter is aimed at alleviating the impact of collisions. This work employs a graphical model for describing the multiuser system which, in turn, facilitates the inclusion of general coding schemes. Based on factor graph representation of the system, several iterative multiuser detectors are presented. These detectors are applicable for any binary linear coding scheme. The performance of the proposed multiuser detectors is evaluated via simulations revealing large gains with low complexity.

Keywords -

I. INTRODUCTION

Impulse-radio systems use short baseband pulses. In Time-Hopping Impulse Radio (TH-IR) systems the information is encoded in the polarity of the pulses (Pulse amplitude modulation - PAM), or in the position of the pulses (Pulse position modulation - PPM). To support multiple access, additional delay is introduced per pulse. The added delay, which is unique for each user, is (pseudo) random, and is assumed to be known to the receiver. Additionally, in order to improve performance, each information bit is typically transmitted several times. As a result of the above measures, the probability of catastrophic collision (multiple-user interference) is minimized. In-depth treatment of Impulse Radio communications is given by Win and Scholtz [1]. While *impulse radio* is typically associated with Radio-Frequency (RF) communications, Visible Light Communications (VLC) is yet another data communication technique that can employ short (light) pulses for signalling, and can hence benefit from the algorithms and results presented herein.

TH-IR was analyzed in the past for several channel models and interference types, see e.g. [2], [3], [4]. Scholtz [5] suggested employing this communication scheme for supporting multiple access. The Multiuser interference (MUI) was modeled as Gaussian noise and the receiver employed a matched filter to detect a specific user [5], [1]. Two different receiver architectures were defined: AIRMA (Analog impulse radio multiple access) and DIRMA (Digital IRMA) receivers [6]. In another work [7] the choice of a different time hopping sequence was discussed, a pseudo-chaotic sequence, aimed

at alleviating the MUI problem. Deterministic sequences designed to mitigate MUI altogether were also proposed [8], [9]. To improve system performance and better deal with MUI in the framework of single-user detection, several authors proposed more general coding and modulation schemes, see e.g. [10], [11], [12], [13].

Rather than treating the signals received from the many users as interference, one can benefit by performing *MultiUser Detection* (MUD), thus extracting the data associated with all users. In general, MUD is a computationally intensive task. To alleviate this problem, Fishler and Poor [14] suggested using an *iterative* multiuser detector for the simple repetition-based code in order to achieve good performance with low-complexity. Wang *et. al.* [15] suggested using the same iterative detector as [14] with different message passing aimed at reducing computational complexity. Chen *et. al.* [16] used the conventional TH-IR scheme concatenated with low-density parity-check (LDPC) coding for improving system performance. Their receiver employed the standard TH-IR detector followed by an LDPC decoder. Sathish *et. al.* [17] proposed using the standard TH-IR scheme concatenated with convolutional coding. The receiver employed an iterative soft-input soft-output, 3-stage multiuser detector. The aforementioned contributions relating to MUD employ concatenation of the standard TH-IR scheme with coding. It would be interesting to introduce advanced coding [18] and multiuser detection techniques for further improving system performance.

LDPC codes were originally introduced by Gallager [19], [20] in 1962, and "reintroduced" in recent years. It was the introduction of Turbo convolutional Codes with efficient iterative decoding (which exhibit notably low error probabilities at low SNR) that triggered the search for such codes - including LDPC codes on this family of codes (see e.g. [21] [22] [23]).

In this paper we present several iterative multiuser receivers for the original TH-IR system. Then, we study a modified system where all users employ arbitrary linear coding, and generalize the above multiuser receiver for this setting. The proposed receivers are based on *factor graph* representation of the complete system. Comparison with the classical repetition-based systems reveal the significant improvements possible with the proposed practical approach. The rest of this manuscript is organized as follows. Section II reviews the system model. In Section III we present iterative multiuser detectors. Finally, Section IV provides simulation results for

the detectors introduced in the previous section using several codes including LDPC codes. Some of the results reported herein appeared in [24].

II. SYSTEM MODEL

A typical UWB TH-IR signal can be described by the following general model:

$$s_{tr}^{(k)}(t) = \sum_{j=-\infty}^{\infty} b_{[j/N_f]}^k w_{tr}(t - jT_f - c_j^k T_c), \quad (1)$$

where $S_{tr}^{(k)}$ is the transmitted signal of the k 'th user; T_f is the nominal pulse repetition time; w_{tr} is the transmitted pulse shape; b_i^k is the i th symbol transmitted by user k ; c_j^k is the time hopping sequence used by user k ; N_f is the number of frames in which a symbol is transmitted; T_c is the chip size.

A user repeats every information symbol in N_f different frames, where each frame consists of N_c chips, also referred to as *slots*. The time hopping sequence employed by each user is a set of values chosen randomly from $\{0, 1, \dots, N_c - 1\}$. Usually $N_c < T_f/T_c$ for avoiding inter-symbol-interference (ISI). In this work the information symbols are assumed to be binary digits (bits) and the signaling is binary-phase shift keying (BPSK).

The system consists of K transmitting users and one receiver, where the different users are centrally coordinated and synchronized by the receiver (base station) [25], [26], [27].

The channel over which the signal is transmitted can be frequency selective; it is assumed that the combined response of the channel and pulse shape is such that the inter-symbol interference is negligible, and the channel characteristics are slowly varying in time. The received signal is perturbed by additive white Gaussian noise (AWGN).

The received signal is given by

$$r(t) = \sum_{k=1}^K A_k \sum_{j=-\infty}^{\infty} b_{[j/N_f]}^k w_{rx}(t - jT_f - c_j^k T_c) + n(t), \quad (2)$$

where K denotes the number of users in the system; w_{rx} is the received waveform associated with one transmitted pulse; A_k is the amplitude associated with user k ; $n(t)$ denotes an additive white Gaussian noise process.

In particular, this channel model can be encountered in scenarios where the dominant propagation path is the line-of-sight, and T_c is chosen to satisfy $T_c > \text{Sup}\{w_{rx}\}$, where $\text{Sup}\{\cdot\}$ is the support of the received pulse w_{rx} . See also [14] and the references therein.

A. Discrete Time model

The receiver tracks the gains associated with the different users. The received signal (2) goes through a matched filter whose output is sampled every T_c seconds. Denote by $\mathbf{r}[i]$ the vector of samples at the output of the matched filter corresponding to the i th information symbol. The size of this vector is $N_f N_c$ and it can be described by the following equation

$$\mathbf{r}[i] = \mathbf{S}[i] \mathbf{A} \mathbf{b}[i] + \mathbf{n}[i], \quad (3)$$

where $\mathbf{S}[i]$ is a $[N_c N_f \times K]$ matrix describing the slots used by the different users for transmitting their i 'th information symbol. The matrix is defined by

$$\mathbf{S}[i]_{lk} = \begin{cases} 1 & \text{if } c_{(i-1)N_f + \lfloor \frac{l}{N_c} \rfloor N_c}^k = l - \lfloor \frac{l}{N_c} \rfloor N_c \\ 0 & \text{otherwise.} \end{cases} \quad (4)$$

\mathbf{A} is the gain between the k 'th transmitter and the receiver, $\mathbf{A} = \text{diag}(A_1, A_2, \dots, A_K)$; $\mathbf{b}[i]$ is the information vector transmitted by the K users at the i 'th interval, $\mathbf{b}[i] = [b_i^1, b_i^2, \dots, b_i^K]^T$; \mathbf{n} is a zero-mean Gaussian random vector with correlation matrix $\sigma_n^2 I$, where $\sigma_n^2 = \frac{N_0}{2}$.

Without loss of generality we can examine the first information symbol and therefore omit the time index i , consequently (3) can be rewritten as

$$\mathbf{r} = \mathbf{S} \mathbf{A} \mathbf{b} + \mathbf{n}. \quad (5)$$

Figure 1 depicts a toy example of transmitting one information symbol in a 2-user system with the following parameters: $N_f = 3$ frames, $N_c = 5$ chips per frame. The rectangles represent the slots used by the users.

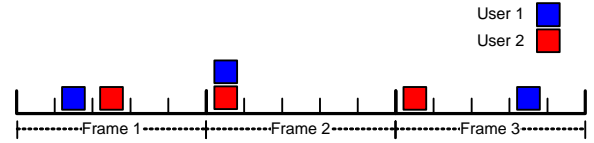


Fig. 1. System illustration

III. ITERATIVE MULTIUSER DETECTION FOR TH-IR SYSTEMS

A major drawback of optimum Multi User Detection (MUD) is implementation complexity. In this section we try to alleviate this problem by presenting several iterative detectors of reduced complexity.

We first introduce a simple iterative detector for the original TH-IR system settings presented in Section II. Then, we propose a graph-based description of the same system, and develop the corresponding MAP-based iterative detector. Finally, we introduce coding into the original system and develop the appropriate graph-based iterative multi-user detector.

A. ID detector

The first detector we present is a (very) low complexity iterative detector based on intuition, rather than mathematical arguments. It is therefore referred to as *ID* (*Intuition-driven*) detector. It is tailored for detecting repetition-based transmissions, and may be characterized as a Gallager-type decoder.

Returning to the toy example of Figure 1, the corresponding \mathbf{S} matrix (4) is given by

$$\mathbf{S}^T = \begin{bmatrix} 0 & 1 & 0 & 0 & 0 & 1 & 0 & 0 & 0 & 0 & 0 & 0 & 1 & 0 \\ 0 & 0 & 1 & 0 & 0 & 1 & 0 & 0 & 0 & 0 & 1 & 0 & 0 & 0 \end{bmatrix}, \quad (6)$$

and the graph we associate with the ID detector is given in Figure 2.

The detector consists of two stages performed in an iterative manner. In the first stage, the estimated value of a specific

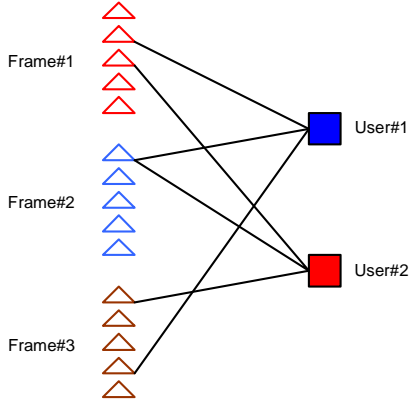


Fig. 2. ID decoder graph: $K = 2$ users, $N_f = 3$ frames, $N_c = 5$ chips per frame.

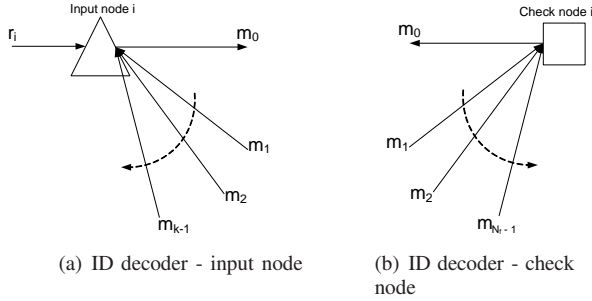


Fig. 3. ID decoder nodes.

pulse is calculated given the received signal and the information transmitted by other colliding users. Associated with the first stage of the decoding is the left-hand side of the graph consisting of at most $N_f N_c$ nodes, one for each of the outputs r of the matched filter. We shall hence refer to these nodes as *input nodes*.

In the second stage, the estimated value of a bit associated with a specific user is calculated given the information from the first stage. The second stage uses the fact that all the pulses of the k th user correspond to the same bit. The right hand side of the graph is associated with the second stage of the decoding. It consists of K nodes, referred to as *check nodes*, one for each of the K users.

The connection between the two sets of nodes is determined by the matrix \mathbf{S} - *input node* i is connected to *check node* j , if $S_{ij} = 1$. The messages passed between the nodes will be "hard" (binary valued), rather than "soft" (e.g. LLR).

We shall now provide a quantitative description of the ID detector beginning with the input nodes, one of which is depicted in Figure 3(a). Without loss of generality consider an output message passed via the first edge. Let m_0 denote the output message, while $m_j, j \neq 0$, denote all the input messages, and r_i is the output of the matched filter connected to input node i . Note that an input node is connected to k check nodes, $0 \leq k \leq K$ being the number of users choosing to transmit in chip position i

$$k = \sum_{l=1}^K S_{i,l}. \quad (7)$$

The output message passed to the check node is defined as

$$m_0 = r_i - \sum_{l=1}^{k-1} A_{i,l} * m_l, \quad (8)$$

where $A_{i,l}$ is the amplitude of user l as seen by input node i .

With the aid of Figure 3(b), we proceed to describe the check nodes. Any check node is connected to exactly N_f input nodes (due to the repetition nature of the transmission). The message computed by a check node (to be passed back to an input node) is defined as

$$m_0 = \text{sgn}\left(\sum_{l=1}^{N_f-1} m_l\right). \quad (9)$$

Note that for the first iteration, the output from all check nodes is initialized to zero. Finally, after the last iteration, the output of the detector is taken from the check nodes, yet it includes all the inputs as follows

$$\hat{b}_k = \text{sgn}\left(\sum_{l=0}^{N_f-1} m_l\right). \quad (10)$$

B. 3-stage Factor-Graph (FG3) detector

In this section we present an iterative (soft) detector based on a 3-stage factor-graph description of the system. While the proposed detector is aimed at decoding the repetition-based transmission, it is of great interest as it lays the ground for introducing arbitrary linear coding into the system.

Henceforth, we let \mathbf{y} represent the received vector \mathbf{r} , i.e. $\mathbf{y} = \mathbf{r}$. The output of the MAP decoder (for the k th bit) is given by

$$\begin{aligned} \hat{b}^k &= \underset{b^k = \pm 1}{\text{argmax}} \{p(b^k | \mathbf{y})\} \\ &= \underset{b^k = \pm 1}{\text{argmax}} \left\{ \sum_{-b^k} p(\mathbf{y} | \mathbf{b}) * \frac{p(\mathbf{b})}{p(\mathbf{y})} \right\}, \end{aligned} \quad (11)$$

where \sum_{-b^k} denotes summing over all values of the vector \mathbf{b} excluding those containing $-b^k$. Since all input vectors, $\{\mathbf{b}\}$ are equiprobable,

$$\begin{aligned} \hat{b}^k &= \underset{b^k = \pm 1}{\text{argmax}} \left\{ \sum_{-b^k} p(\mathbf{y} | \mathbf{b}) \right\} \\ &= \underset{b^k = \pm 1}{\text{argmax}} \left\{ \sum_{-b^k} p(\mathbf{y} | b^1, \dots, b^K) \right\}. \end{aligned} \quad (12)$$

Using the following definition

$$\mathbb{E}(x_1, \dots, x_i) = \begin{cases} 1 & \text{if } x_1 = \dots = x_i \\ 0 & \text{otherwise} \end{cases}, \quad (13)$$

one can write

$$\begin{aligned} \hat{b}_j^k &= \underset{b_j^k = \pm 1}{\text{argmax}} \left\{ \sum_{-b^k} p(\mathbf{y} | b_0^1, \dots, b_{N_f-1}^1, \dots, b_K^1, \dots, b_{N_f-1}^K) \right. \\ &\quad \cdot \prod_{k=1}^K \mathbb{E}(b_0^k, \dots, b_{N_f-1}^k) \left. \right\}. \end{aligned} \quad (14)$$

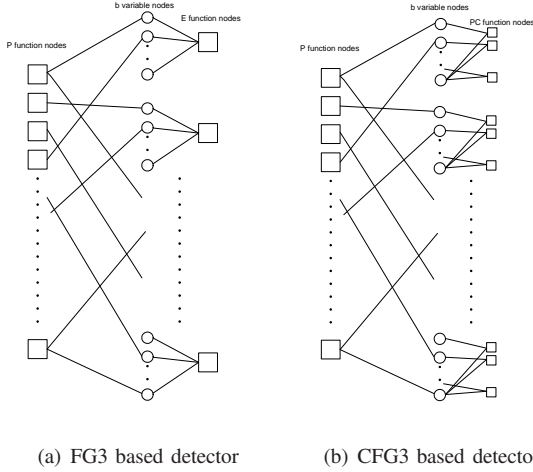


Fig. 4. Factor graph representation used for multiuser detection - Repetition code example.

Note that the subscript j , denoting the frame index, has been added though one expects all N_f estimations $\hat{b}_j^k, j \in \{0, 1, \dots, N_f - 1\}$ to produce the same value.

Since the channel is memoryless

$$p(\mathbf{y}|b_0^1, \dots, b_{N_f-1}^1, \dots, b_K^1, \dots, b_{N_f-1}^K) = \prod_{i=1}^{N_f N_c - 1} p(y_i | b_{yi}), \quad (15)$$

where b_{yi} represents the transmitted bits from all users employing chip slot i . Finally, we have

$$\hat{b}_j^k = \operatorname{argmax}_{b_j^k = \pm 1} \left\{ \sum_{-b^k}^{N_f N_c - 1} \prod_{i=1}^{N_f N_c - 1} p(y_i | b_{yi}) \prod_{k=1}^K \mathbb{E}(b_0^k, \dots, b_{N_f-1}^k) \right\}. \quad (16)$$

This, so-called, "sum-of-products" function can be calculated using a message passing algorithm operating iteratively on a bipartite graph, termed *factor graph* [28], [29]. A factor graph typically consists of two types of nodes - *function nodes* and *variable nodes*. In Figure 4(a) we depict a graph corresponding to Equation (16).

The graph consists of three types of nodes. The squares represent function nodes, which are divided into two types. The first type of function nodes are associated with the function $p(y_i | b_{yi})$; there are exactly $N_f N_c$ such nodes. We shall denote these as *P function nodes*. The second type of function nodes are associated with $\mathbb{E}(b_0^k, \dots, b_{N_f-1}^k)$; there are exactly K such nodes. Denote this type of nodes as *E function nodes*. Nodes indicated by circles represent the variable nodes for b_j^k ; there are exactly $K N_f$ such nodes. Denote these nodes as *b variable nodes*. Note that the edges connecting the *P function nodes* with the *b variable nodes* are completely defined by the matrix S . Finally, as will be shown later on, by omitting the *b variable nodes*, the graph reduces to the one shown for the ID detector.

The messages passed by the algorithm shall be denoted by $\mu(x)$, $x = \pm 1$. $\mu_{p \rightarrow v}$ represents a message passed from a *P function node* to a *b variable node*, $\mu_{v \rightarrow E}$ represents a message from *b variable node* to *E function node*, while $\mu_{E \rightarrow v}$ is a message from *E function node* to *b variable node*. Next, we

provide explicit description of the messages associated with the different types of nodes.

1) *P function nodes*: The $\mu_{p \rightarrow v}$ messages, calculated at the *P function nodes*, are

$$\begin{aligned} \mu_{p \rightarrow v}(+1) &= \sum_{x_1, \dots, x_J} p(y|+1, x_1, \dots, x_J) \prod_{j=1}^J \mu_j(x_j); \\ \mu_{p \rightarrow v}(-1) &= \sum_{x_1, \dots, x_J} p(y|-1, x_1, \dots, x_J) \prod_{j=1}^J \mu_j(x_j), \end{aligned} \quad (17)$$

where x_i is a binary value conveyed by an edge connected to an adjacent variable node. W.l.o.g. $\mu(\pm 1)$ denotes the output message passed to the variable node of index 0, while $\mu_j(x_j)$ denotes an input message originating at an adjacent *b variable node*. (There are J input edges, with j being the edge index.) We shall henceforth omit the cumbersome directive pointers, $p \rightarrow v$ and $v \rightarrow p$, as it will always be easy to realize the correct flow.

Rather than passing two messages, one may use a single message in the form of the log likelihood ratio (LLR). Let r be defined as follows

$$\begin{aligned} r &\equiv \frac{\mu(+1)}{\mu(-1)} \\ &= \frac{\sum_{x_1, \dots, x_J} p(y|1, x_1, \dots, x_J) \prod_{j=1}^J \mu_j(x_j)}{\sum_{x_1, \dots, x_J} p(y|-1, x_1, \dots, x_J) \prod_{j=1}^J \mu_j(x_j)} \\ &= \frac{\sum_{x_1, \dots, x_J} p(y|1, x_1, \dots, x_J) \prod_{j=1}^J \mu_j(x_j) \frac{1}{\mu_j(-1)}}{\sum_{x_1, \dots, x_J} p(y|-1, x_1, \dots, x_J) \prod_{j=1}^J \mu_j(x_j) \frac{1}{\mu_j(-1)}}. \end{aligned} \quad (18)$$

Note that

$$\frac{\mu_j(x_j)}{\mu_j(-1)} = r_j^{\frac{x_j+1}{2}}. \quad (19)$$

Finally, using (19) the LLR, $l = \log(r)$, is given by

$$l = \log \frac{\sum_{x_1, \dots, x_J} p(y|1, x_1, \dots, x_J) \prod_{j=1}^J e^{l_j \frac{x_j+1}{2}}}{\sum_{x_1, \dots, x_J} p(y|-1, x_1, \dots, x_J) \prod_{j=1}^J e^{l_j \frac{x_j+1}{2}}}. \quad (20)$$

2) *b variable nodes*: It is easy to see that each of the *b variable nodes* is connected to exactly one *P function node* on the left and one *E function node* on the right. In this case the output messages are the same as the input messages.

3) *E function nodes*: For this type of nodes we have

$$\begin{aligned} r &= \frac{\sum_{x_1, \dots, x_{N_f-1}} \mathbb{E}(1, x_1, \dots, x_{N_f-1}) \prod_{j=1}^{N_f-1} \mu_j(x_j)}{\sum_{x_1, \dots, x_{N_f-1}} \mathbb{E}(-1, x_1, \dots, x_{N_f-1}) \prod_{j=1}^{N_f-1} \mu_j(x_j)} \\ &= \frac{\sum_{x_1, \dots, x_{N_f-1}} \mathbb{E}(1, x_1, \dots, x_{N_f-1}) \prod_{j=i}^{N_f-1} r_j^{\frac{x_j+1}{2}}}{\sum_{x_1, \dots, x_{N_f-1}} \mathbb{E}(-1, x_1, \dots, x_{N_f-1}) \prod_{j=i}^{N_f-1} r_j^{\frac{x_j+1}{2}}}. \end{aligned} \quad (21)$$

Recalling the definition of \mathbb{E} , (13), it is easily verified that

$$\begin{aligned} r &= \frac{\prod_{j=1}^{N_f-1} r_j^{\frac{1+1}{2}}}{\prod_{j=1}^{N_f-1} r_j^{\frac{1+1}{2}}} \\ &= \prod_{j=1}^{N_f-1} r_j, \end{aligned} \quad (22)$$

and the LLR is simply

$$l = \log(r) = \sum_{j=1}^{N_f-1} l_j. \quad (23)$$

After the last iteration is performed, the output of the detector is taken from the *E function node*:

$$\hat{b}^k = \text{sgn}\left(\sum_{j=1}^{N_f} l_j\right). \quad (24)$$

We described a multiuser detector based on factor graph representation of the system. Recall that Fishler and Poor (FP) [14] presented an iterative multiuser detector for the same system that follows the turbo principle. Interestingly, the FG3 detector turns out to be the same as the FP detector although a different model is employed for describing the system. This assertion may not be obvious by simply comparing at the message passing equations. However, by using simple mathematical manipulations one can move from the set of equations presented herein to those used by FP. It can be shown that the FP and FG3 detectors are not MAP-achieving since the associated graphs are not cyclic-free.

C. CFG3 detector

The FG3 proposed model and detection technique shall now serve as the basis for the introduction of a coded system. The receiver to be developed in this section is aimed at providing a solution for a system employing arbitrary linear coding. It shall hence be denoted as coded-FG3 (CFG3).

A linear code is typically defined by its parameters $[n, k, d]$, where n is the code length, k is the dimension of the code (not to be confused with the number of users), and d denotes the minimum Hamming distance of the code. Hence, in a coded TH-IR system, the number of frames N_f will satisfy $N_f = n$, and the system rate is $\frac{k}{n}$.

Referring to Equation (16), the function $\mathbb{E}(\cdot)$ represents the fact that the bits associated with a specific user must all be the same. When a code $[n, k, d]$ is used, we shall replace $\mathbb{E}(\cdot)$ with a new function, $\mathbb{P}\mathbb{C}$, representing a Parity Check equation.

The parity check matrix \mathbf{H} is an $(n - k) \times n$ binary matrix

$$\mathbb{P}\mathbb{C} = \prod_{i=1}^{n-k} PC_i, \quad (25)$$

where PC_i is defined as follows

$$\mathbb{P}\mathbb{C}_i = \begin{cases} 1 & \text{if } (\sum_{j, h_{i,j}=1} b_j) = 1 \text{ where the sum is over GF2} \\ 0 & \text{otherwise} \end{cases} \quad (26)$$

As an example, Figure 4(b) depicts a factor graph of a linear code when the latter is a repetition code whose parity check matrix \mathbf{H} is given by

$$\mathbf{H} = \begin{pmatrix} 1 & 0 & 0 & \dots & 1 \\ 0 & 1 & 0 & \dots & 1 \\ \vdots & \vdots & \ddots & & \\ 0 & 0 & \dots & 1 & 1 \end{pmatrix}.$$

Although this graph is different from Figure 4(a), which means that two different detectors are to be used, both graphs target the same system and code.

The *b variable nodes* have one input (from the left), but typically several outputs (connected to PC function nodes). The messages to be calculated and passed to the output are

$$\begin{aligned} \mu(1) &= \prod_i \mu_i(1) \\ \mu(-1) &= \prod_i \mu_i(-1), \end{aligned} \quad (27)$$

and hence

$$\begin{aligned} r &= \frac{\mu(1)}{\mu(-1)} = \prod_i r_i \\ l &= \log(r) = \sum_i l_i. \end{aligned} \quad (28)$$

The messages to be calculated at the *PC function nodes* are associated with single parity check equations. These are the same messages used in LDPC decoding:

$$l = 2 \tanh^{-1}\left(\prod \tanh \frac{l_j}{2}\right). \quad (29)$$

After iterating all messages through the graph, the final marginalization is performed at the *b variable nodes*

$$\hat{b}^k = \text{sgn}\left(\sum_j l_j\right). \quad (30)$$

It can be shown that by appropriately choosing the code, the associated graph can be made cyclic-free, and hence CFG3 is MAP-achieving.

IV. SIMULATION RESULTS

A. Conventional repetition-based system

We first study the original system employing a repeated transmission scheme. We shall consider two different detectors: the FG3 detector and the CFG3 detector. In all presented simulations the number of slots per frame is $N_c = 20$, while the number of users varies, $K = \{3, 10, 30\}$.

Figures 5 hold the simulation results. The performance of the FG3 and the CFG3 detectors are practically the same. Therefore, whenever using repetition-based coding, we shall only consider the FG3 detectors.

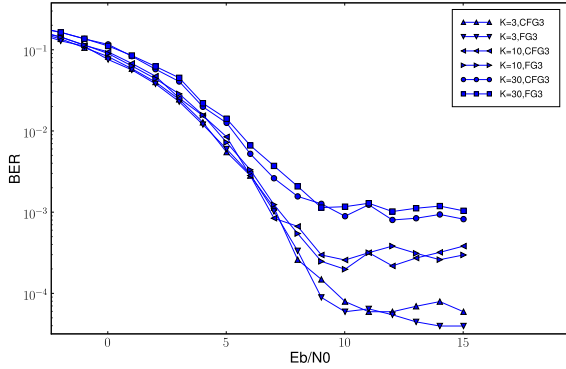


Fig. 5. Repetition-based system, FG3 and CFG3 detectors, $N_c = 20$

B. Repetition vs. LDPC-based systems

We next compare the performance of a repeated transmission system (using ID and FG3 detectors) with an LDPC-based coded system (using CFG3 detector). The parameters of the LDPC code chosen are $(n = 120, k = 56, R = 0.4667)$ - Mackay code 120.64.3.109 [30]. It has been chosen because of its relatively short length¹; no attempt has been made to optimize it for our system. Repetition code of rate $\frac{1}{3} \rightarrow N_f = 3$ have been chosen for comparison.

Figures 6 and 7 pertain to the repetition code with ID and FG3 detectors, respectively, while Figure 8 pertains to the LDPC code-based system employing the CFG3 detector. The ID and FG3 detectors exhibit an error floor which is irreducible due to the fact that system performance is limited by Multi User Interference (MUI). To support this assertion note how the error floor increases with the number of users. The FG3 detector exhibits better error floor performance than the ID detector, as expected.

Clearly, the LDPC-based system with the CFG3 detector behaves differently. First, the BER curve is much sharper as might be expected of a coded system. Second, as demonstrated in Figure 8, when the number of users increases, the E_b/N_0 threshold-point also increases. Still, once the threshold is passed, the slopes associated with all cases are similar. Increasing the number of users amounts to adding more noise, which leads us to the next observation: another threshold that can be clearly identified corresponds to the number of users - beyond a certain number of users, the system collapses.

In general, we argue that the LDPC-based system handles MUI much better than the alternative approaches mainly because it employs a large number of frames (N_f). Consequently, "catastrophic" collisions among different users are much less common.

Complexity-wise we argue as follows. ID performs only simple addition operations. Calculation of the message at the input node (8) requires $O(K^i)$ additions, where K^i is the number of colliding users. Check node calculation (9) requires $O(N_f)$ additions. Recall that the graphs associated with the ID and FG3 systems are the same. The two detectors differ only

¹Recall that the number of frames, N_f , in our system model is actually the code length. Since the total number of time slots in the system is $N_f N_c$, reasonable simulation times are when using shorter codes.

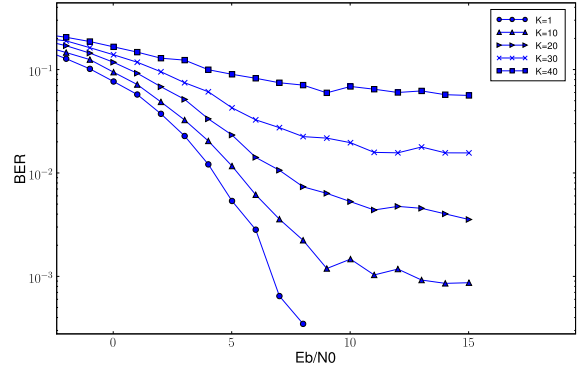


Fig. 6. ID detector, Repetition, $N_f = 3$, $N_c = 20$

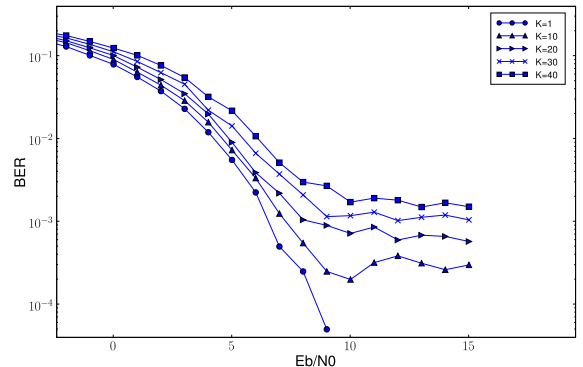


Fig. 7. FG3 detector, Repetition, $N_f = 3$, $N_c = 20$

in the calculations carried out at the input nodes. Calculating (20), instead of (8), increases complexity by $O(2^{K^i})$ [14]. Moving from FG3 to CFG3, as the input nodes remain the same, the added complexity is that of decoding. In our example, LDPC coding has been employed, and therefore the additional complexity is given by $C_{LDPC} \cdot K$, where C_{LDPC} is the complexity required for decoding the LDPC code used.

Compared to ID, FG3 better treats MUI for the price of increased complexity at the input side (left-hand side of the graph). CFG3 add coding gain for the price of increased complexity at the coding side (right-hand side of the graph). In conclusion, among the three described schemes (for the same E_b/N_0), the LDPC-based system provides the best performance both in terms of BER and overall system throughput.

C. Performance dependency on the number of users

In a multi-user environment users often join and leave the system. Analyzing the performance of the system for different numbers of users is therefore of interest.

A system with $N_c = 20$ slots per frame is considered: ID and FG3 detectors are employed for a repetition-based transmission scheme with $N_f = 3$ ($rate = 1/3$); CFG3 detector with LDPC code $(n = 120, k = 56, R = 0.4667)$ is also considered.

Figures 9 and 10 present the simulation results for $E_b/N_0 = 20dB$ and $E_b/N_0 = 5dB$, respectively. For $E_b/N_0 = 20dB$,

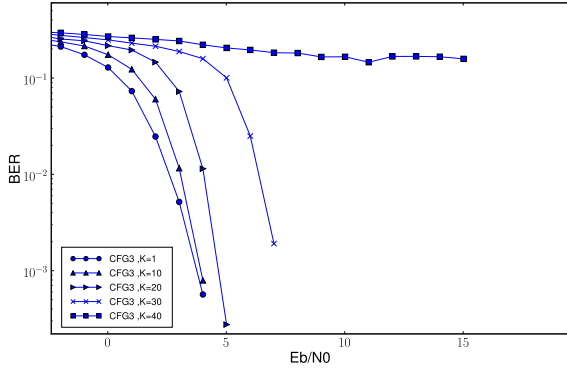


Fig. 8. CFG3 detector, LDPC, ($n = 120, k = 56, R = 0.4667$), $N_c = 20$

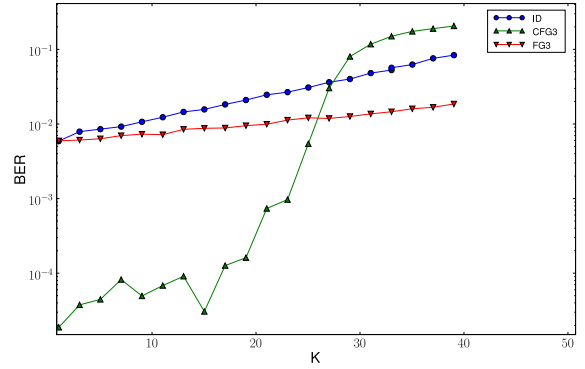


Fig. 10. Multi-User Performance, $E_b/N_0 = 5dB$

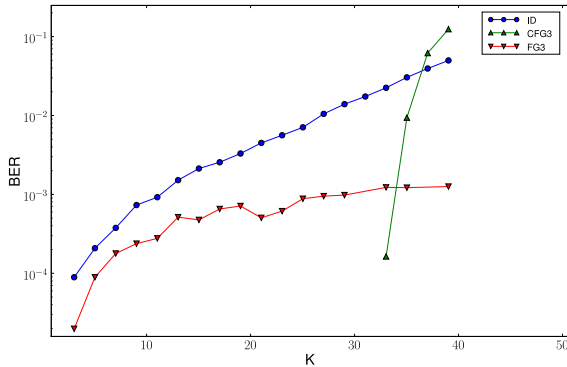


Fig. 9. Multi-User Performance, $E_b/N_0 = 20dB$

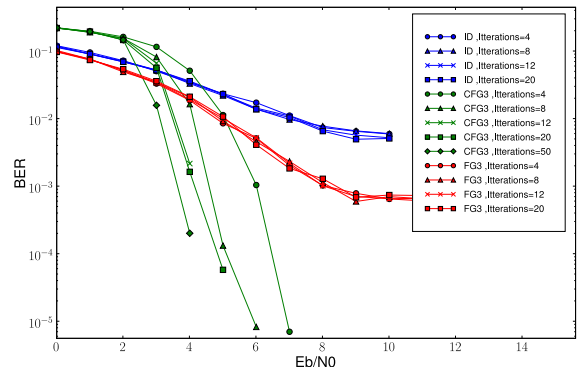


Fig. 11. Performance dependency on number of iterations, $K = 20$ users

MUI is the dominant impairment. The performance of the ID and FG3 detectors gradually deteriorate as the number of users is increased from 3 to 40. FG3 exhibits better behavior throughout. The LDPC coded system with CFG3 detector performs quite differently. No errors are observed until the number of users reaches a certain threshold, 33 in this simulation. Once the threshold is passed, performance degradation is steep. Exact position of the threshold and its behavior depend on system parameters.

In the second simulation, shown in Figure 10, the additive noise is not negligible. The CFG3 detector behaves much like before: as long as the number of users is below a certain threshold, performance degradation is quite moderate. Also notice that the threshold moved to the left due to the existence of noticeable noise. The ID and FG3 detectors perform much worse than the CFG3 detector with FG3 being only slightly superior to the ID detector.

D. Performance dependency on iterations

The influence of the number of iterations on performance has so far been overlooked; a fixed number of 8 iterations was used throughout. Notably, increasing the number of iterations benefits the LDPC-based system more than the alternatives.

As an illustrative example Figure 11 presents the BER performance of the three detectors, as a function of E_b/N_0 , for $K = 20$ users and different number of iterations. The performance of the ID and FG3 detectors converge in only

4 iterations. More iterations are required for the LDPC-based system to converge. In the single-user case (simulation results not shown), the number of iterations required for the LDPC-based system to converge is smaller than in the multi-user case. One may argue that this follows from the fact that the graph associated with the multi-user case is much more involved.

E. Some after simulation comments

In a single-user system, the user can clearly employ all the time slots for its own usage. In the case of high SNR, with two-level modulation, the channel capacity is upper bounded by $1[\text{bit}/\text{chip}]$. Since each frame provides N_c transmit opportunities, the capacity of the single-user system is upper bounded by $C = N_c[\text{bits}/\text{frame}]$. Let us now consider the CFG3-based system with K users. The code rate used was 0.46 and $N_c = 20$. The CFG3 detector hardly produced any bit errors as long as the number of users satisfied $K < 33$. The overall system throughput in this case is $C = 14.72[\text{bits}/\text{frame}]$ as compared to the above upper bound of $C = N_c = 20[\text{bits}/\text{frame}]$. With an optimized LDPC code of greater length, the obtained throughput is expected to grow closer to this bound.

V. CONCLUSIONS

This work is concerned with iterative receivers for a multiuser TH-IR system. In particular, we study the gain achieved

by introducing coding into the originally uncoded system. Several iterative multi-user detectors have been presented based on factor graph representation of the complete system. These detectors are general and can support any binary linear coding scheme. Yet another strength of the proposed approach is that the graph used may be extended to account for multipath components (owing to the nature of the UWB channel). This is an interesting topic for future work.

Simulation results for the above mentioned detectors are presented for several codes including LDPC codes. It is demonstrated that for 20 users, BER of 10^{-3} can be achieved with higher system rate and more than $4dB$ gain in E_b/N_0 when using an LDPC-coded system. Furthermore, it is shown that the achievable performance of the original system quickly saturates at relatively poor BER.

REFERENCES

- [1] M.Z. Win and R.A. Scholtz. Impulse radio: how it works. *Communications Letters, IEEE*, 2(2):36–38, Feb 1998.
- [2] I. Bergel, E. Fishler, and H. Messer. Narrowband interference suppression in time-hopping impulse-radio systems. In *Ultra Wideband Systems and Technologies. Digest of Papers. 2002 IEEE Conference on*, pages 303–307, 2002.
- [3] Li Zhao and A.M. Haimovich. Performance of ultra-wideband communications in the presence of interference. *Selected Areas in Communications, IEEE Journal on*, 20(9):1684–1691, Dec 2002.
- [4] F. Ramirez-Mireles. On the performance of ultra-wide-band signals in gaussian noise and dense multipath. *Vehicular Technology, IEEE Transactions on*, 50(1):244–249, Jan 2001.
- [5] R. Scholtz. Multiple access with time-hopping impulse modulation. In *Military Communications Conference, 1993. MILCOM '93. Conference record. 'Communications on the Move'.*, IEEE, volume 2, pages 447–450 vol.2, Oct 1993.
- [6] M.Z. Win and R.A. Scholtz. Ultra-wide bandwidth time-hopping spread-spectrum impulse radio for wireless multiple-access communications. *Communications, IEEE Transactions on*, 48(4):679–689, Apr 2000.
- [7] D.C. Laney, G.M. Maggio, F. Lehmann, and L. Larson. Multiple access for uwb impulse radio with pseudochaotic time hopping. *Selected Areas in Communications, IEEE Journal on*, 20(9):1692–1700, Dec 2002.
- [8] C.J. Le Martret and G.B. Giannakis. All-digital impulse radio with multiuser detection for wireless cellular systems. *Communications, IEEE Transactions on*, 50(9):1440–1450, Sep 2002.
- [9] Liuqing Yang and G.B. Giannakis. Block-spreading codes for impulse radio multiple access through isi channels. In *Communications . ICC 2002. IEEE International Conference on*, volume 2, pages 807–811 vol.2, 2002.
- [10] Xiaoli Chu and R.D. Murch. Multidimensional modulation for ultra-wideband multiple-access impulse radio in wireless multipath channels. *Wireless Communications, IEEE Transactions on*, 4(5):2373–2386, Sept. 2005.
- [11] Yafei Tian and Chenyang Yang. Coded modulation in uwb communications. In *Personal, Indoor and Mobile Radio Communications, 2005. PIMRC 2005. IEEE 16th International Symposium on*, volume 1, pages 491–495, Sept. 2005.
- [12] Youn Seok Kim, Won Mee Jang, and Lim Nguyen. Self-encoded thppm uwb system with iterative detection. In *Advanced Communication Technology, 2006. ICACT 2006. The 8th International Conference*, volume 1, pages 5 pp.–714, Feb. 2006.
- [13] H. Zhang, W. Li, and T.A. Gulliver. Pulse position amplitude modulation for time-hopping multiple-access uwb communications. *Communications, IEEE Transactions on*, 53(8):1269–1273, Aug. 2005.
- [14] E. Fishler and H.V. Poor. Low-complexity multiuser detectors for time-hopping impulse-radio systems. *Signal Processing, IEEE Transactions on*, 52(9):2561–2571, Sept. 2004.
- [15] Bao-Yun Wang and Wei Xing Zheng. Multiuser detection for time-hopping impulse-radio systems using a low-complexity iterative algorithm.
- [16] Fangni Chen, Shiju Li, and Lei Shen. Performance evaluation of a novel low-density parity-check coded ultra wide band impulse radio (uwb-ir) system. In *Wireless Communications, Networking and Mobile Computing, 2006. WiCOM 2006. International Conference on*, pages 1–4, Sept. 2006.
- [17] A.D. Sathish and S.K. Jayaweera. Iterative low-complexity multiuser detection and decoding for coded uwb systems. In *Spread Spectrum Techniques and Applications, 2006 IEEE Ninth International Symposium on*, pages 173–177, Aug. 2006.
- [18] Chia-Chin Chong, F. Watanabe, and H. Inamura. Potential of uwb technology for the next generation wireless communications. In *Spread Spectrum Techniques and Applications, 2006 IEEE Ninth International Symposium on*, pages 422–429, Aug. 2006.
- [19] R. Gallager. Low-density parity-check codes. *Information Theory, IRE Transactions on*, 8(1):21–28, January 1962.
- [20] R. Gallager. *Low Density Parity Check Codes*. M.I.T. Press, Cambridge, Massachusetts, 1963.
- [21] D.J.C. MacKay. Good error-correcting codes based on very sparse matrices. *Information Theory, IEEE Transactions on*, 45(2):399–431, March 1999.
- [22] T.J. Richardson and R.L. Urbanke. The capacity of low-density parity-check codes under message-passing decoding. *Information Theory, IEEE Transactions on*, 47(2):599–618, February 2001.
- [23] T.J. Richardson, M.A. Shokrollahi, and R.L. Urbanke. Design of capacity-approaching irregular low-density parity-check codes. *Information Theory, IEEE Transactions on*, 47(2):619–637, February 2001.
- [24] Y.S. Bahar and O. Amrani. Iterative multiuser detection in coded uwb. In *Electrical and Electronics Engineers in Israel. IEEEI 2008. IEEE 25th Convention of*, pages 450–451, Dec. 2008.
- [25] Chee-Cheon Chui and R.A. Scholtz. A synchronizing scheme for an impulse network. In *Military Communications Conference, MILCOM 2004. IEEE*, volume 2, pages 635–641 Vol. 2, Oct.-3 Nov. 2004.
- [26] C. Carbonelli, S. Franz, U. Mengali, and U. Mitra. Semi-blind ml synchronization for uwb transmitted reference systems. In *Signals, Systems and Computers, 2004. Conference Record of the Thirty-Eighth Asilomar Conference on*, volume 2, pages 1491–1495 Vol.2, Nov. 2004.
- [27] E.A. Homier and R.A. Scholtz. Rapid acquisition of ultra-wideband signals in the dense multipath channel. In *Ultra Wideband Systems and Technologies. Digest of Papers. 2002 IEEE Conference on*, pages 105–109, 2002.
- [28] F.R. Kschischang, B.J. Frey, and H.-A. Loeliger. Factor graphs and the sum-product algorithm. *Information Theory, IEEE Transactions on*, 47(2):498–519, Feb 2001.
- [29] H.-A. Loeliger. An introduction to factor graphs. *Signal Processing Magazine, IEEE*, 21(1):28–41, Jan. 2004.
- [30] D.J.C. MacKay. *Encyclopedia of Sparse Graph Codes*. <http://www.inference.phy.cam.ac.uk/mackay/codes/data.html>.